Originally published in *Proceedings of the Fifth International Workshop on Compressible Turbulent Mixing*, ed. R. Young, J. Glimm & B. Boston.
ISBN 9810229100, World Scientific (1996).

Physics of the Strong Shock Richtmyer–Meshkov Instability*

Ravi Samtaney[1,2] and Daniel I. Meiron[1]

[1] 217-50, Applied Mathematics
Caltech, Pasadena, CA 91125

[2] Graduate Aeronautical Laboratories
Caltech, Pasadena, CA 91125

Abstract. The Richtmyer-Meshkov instability is numerically investigated for strong shocks i.e. for hypervelocity cases. To model the interaction of the flow with non-equilibrium chemical effects typical of high-enthalpy flows, the Lighthill-Freeman ideal dissociating gas model is employed. For large Atwood numbers, dissociation causes significant changes in density and temperature, but the change in growth of the perturbations is small. A Mach number scaling for strong shocks is examined. A local analysis is used to determine the initial baroclinic vorticity generation on positive and negative Atwood number interfaces.

1 Introduction

Recently, the Richtmyer-Meshkov instability [5, 3] has been the subject of extensive research, including laboratory experiments and numerical simulations [2]. Hitherto, most investigations of the Richtmyer-Meshkov (RM) instability have been confined to shocks of Mach number, $M \leq 4$. In this paper, we present results for the case of *hypervelocity* RM instability. The term "hypervelocity" is used in distinction with the term "hypersonic". Hypervelocity implies not only high Mach number but also large velocities and therefore high total enthalpy. Thus, in hypervelocity RM instability, the shocks are of strength sufficient to activate dissociation/recombination chemistry and related gas-chemistry interactions.

2 Physical Parameters, Equations and Chemistry Model, and Numerical Method

2.1 Physical Parameters

The physical domain is a two-dimensional rectangular shock tube of dimensions $[x_l, x_r] \times [0, \lambda/2]$. A vertical interface separating two gases is perturbed sinusoidally with wave-

*This work was supported in part by AFOSR grant no. F49620-93-1-0338 and by the Lawrence Livermore National Laboratory under subcontract B295121 under DOE contract W-7405-ENG-48.

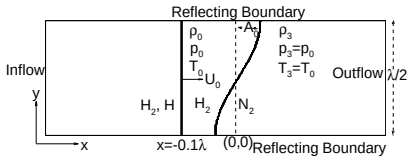

Figure 1: Schematic of the physical domain and parameters.

length $\lambda \equiv 10$cm, and initial amplitude $A_0 = 0.1\lambda$ (see Fig. 1). The interface used is hydrogen-nitrogen (low-high acoustic impedance). The gases are initially in thermal ($T_0 = T_b = 298$ K) and mechanical equilibrium ($p_0 = p_b = 0.1$ atm). Although for chemically active flows, the Mach number is an ill-defined quantity, for convenience we define a Mach number by $M \equiv U_0/c_0$, where U_0, c_0 are the shock speed and the frozen sound speed in the unshocked hydrogen. In fact, for $T_0 = T_b = 298$ K the frozen and equilibrium sound speeds are identical.

2.2 Equations and chemistry model

Consistent with previous studies of the RM instability, the governing equations of motion are the compressible Euler equations in two dimensions. In this paper we examine two limits: (a) *frozen* (Damkohler number $\Omega = 0$); and (b) *equilibrium* ($\Omega \to \infty$). For $\Omega \to \infty$, we assume that the equilibrium chemical reactions are adequately modeled by the Lighthill Ideal Dissociating Gas (IDG) model ([1]). The law of mass action for the IDG model is

$$\frac{\alpha_k^2}{1-\alpha_k} = \frac{\rho_{d,k}}{\rho_k} \exp\left(\frac{-\theta_{d,k}}{T}\right). \tag{1}$$

In Eq.(1), ρ_k is the density of the kth gas ($k = 1, 2$); α_k is the mass fraction of the monatomic constituent of the kth gas; $\theta_{d,k}$ is the dissociation temperature of the kth gas, and $\rho_{d,k}$ is the characteristic density. The IDG properties for hydrogen and nitrogen are: $\rho_d = 1800, 130000$ kg/m^3 and $\theta_d = 51900, 113200$ K. Note that in the IDG model the gas is always in a state of vibrational excitation which implies an incorrect limit of the ratio of specific heats, $\gamma \to 4/3$ at low temperatures.

2.3 Numerical method

The numerical method employed here is a second-order accurate Equilibrium Flux Method (EFM) ([4]). For equilibrium chemistry computations, we employ operator splitting, i.e. the hydrodynamical equations are solved and then the law of mass action

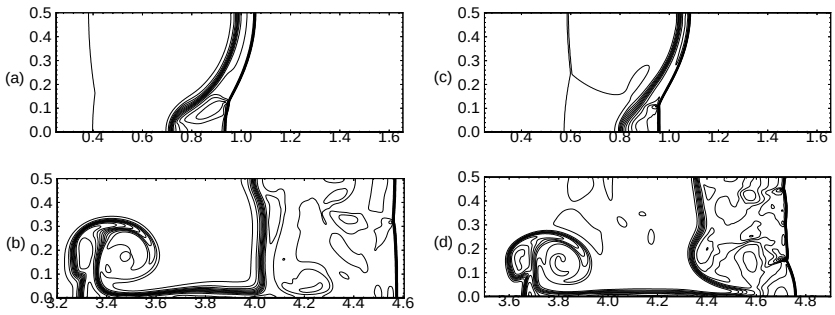

Figure 2: Density contours for an $M = 10$ shock interaction with a H_2-N_2interface at $t = 0.167, 0.88$ for frozen (left column, $\rho = (6.6, 122.0)$) and equilibrium chemistry (right column, $\rho = (8.8, 220)$).

(for $\Omega \to \infty$, Eq. 1) for each gas is solved in every computational cell. The physical domain is subdivided into a uniform 2000×200 grid. A message-passing parallel code was implemented on 512 node Intel Paragon which is a message-passing parallel machine, and achieved roughly 1.4 GFlops performance.

3 Simulation Results

In this section we present results for a $M = 10$ shock interaction with a H_2-N_2 interface perturbed sinusoidally with $A_0/\lambda = 0.1$. For the results presented, the density, velocity, time, and length are normalized by ρ_0, c_0, λ/c_0 and λ respectively. Note that λ/c_0 is the time taken for an acoustic wave to travel one wavelength. The extent of physical domain in the x-direction is $[x_l, x_r] \equiv [-0.2\lambda, 4.8\lambda]$. The first interaction between the shock and the interface is the very rapid shock refraction process. In this case the transmitted and the reflected waves are both shock waves. The transmitted shock moves at a slower speed relative to the incident shock while the reflected shock moves to the right in the laboratory frame of reference. In Figs. 2 and 3 density and vorticity contours are shown at "early" and "late" times during the interaction. During the refraction process, negative vorticity is generated due to *baroclinicity*. As the curved reflected and transmitted shocks straighten, triple points form on the shock fronts due to the nonlinear interactions. Associated with these triple points are shear layers with positive vorticity. As time increases, these triple points traverse the reflected (or transmitted) shock fronts and further reflections from the top and bottom boundaries cause the appearance of shear layers (with alternating signs of vorticity). The contact rolls up and gives rise to the familiar mushroom shaped morphology of the interface. The bubble rapidly assumes a nearly flat shape. This implies that the growth of the

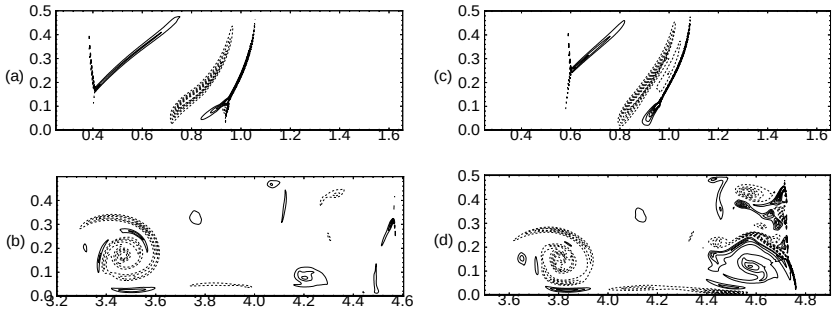

Figure 3: Vorticity contours (dashed negative), $\omega = (-78, 78)$ for frozen (left column) and equilibrium chemistry (right column).

perturbation is mostly due to the relative velocity of the intense spike. The main effect of the endothermic dissociation reaction is to increase the gas density and lower the temperature. The ratio of the peak density (temperature) in the equilibrium chemistry to the frozen chemistry case is approximately 1.7 (0.4). The maximum dissociated fraction of hydrogen (nitrogen) is about 20% (36%). At any instant, the growth rate dA/dt is different for both cases while the amplitude A of the perturbation shows a very small reduction due to dissociation (see Fig. 4). The growth rate given by the impulse model ([5]) over-predicts the true growth rate significantly. In fact, no "linear" period of growth is observed for this case or even for the case with $A/\lambda = 0.01$ (not shown).

The first slope change in the total circulation Γ and the total interfacial circulation Γ_i, (see Fig. 5) occurs when the incident shock has completely traversed the interface. The circulation at this point may be determined by means of a local analysis (see Section 4). The circulation Γ shows strong variation with time due to the generation of the shear layers as explained above. The interfacial circulation changes in large part due to the strong compression waves interacting with the interface. At late times, the difference in Γ_i in the two limiting cases is small.

3.1 Mach Number Scaling

Note that the hydrodynamic equations are invariant under the following transformation:

$$t \to tM, p \to p/M^2, u \to u/M, E \to E/M^2 \tag{2}$$

It is also well-known that for high Mach number perfect gas flows that the pressure and the velocity behind a shock scale quadratically and linearly in Mach number, M. We expect that the above scaling hold for our cases and furthermore we are interested in departure from the above scaling in the presence of chemistry.

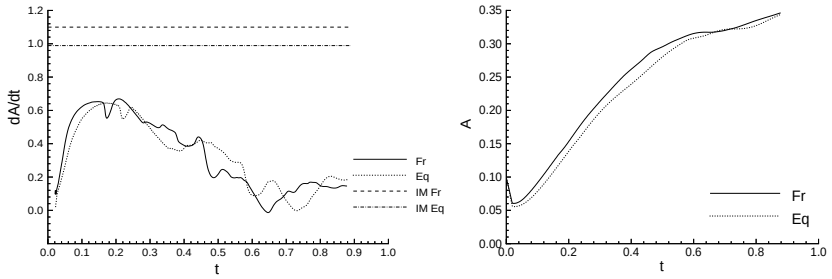

Figure 4: (a) Growth rate and (b) amplitude of the perturbation as a function of time. Eq: Equilibrium, Fr: Frozen chemistry, and IM: Impulse Model. $M = 10$ shock; $A_0/\lambda = 0.1$, H_2-N_2 interface.

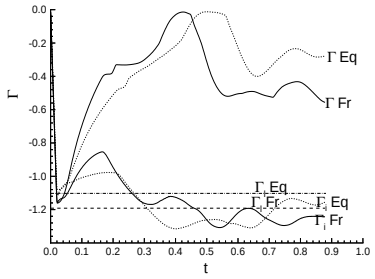

Figure 5: Total circulation Γ, and interfacial circulation Γ_i as a function of time. Γ_l is circulation from a local analysis. $M = 10$ shock; $A_0/\lambda = 0.1$, H_2-N_2 interface

In Fig. 6 the amplitude is plotted as a function of tM i.e. time scaled by the Mach number of the shock for both the frozen and the equilibrium case.

4 Local Analysis

Consider a sawtooth perturbed interface inclined at an angle β_0 to the plane of the incident shock (Fig. 7). Extending previous work ([6]) for $\Omega = \infty$ we obtain the solution for small β_0 in a small neighborhood of the node where all the waves meet.

For $\beta_0 = 30^o$ and a H_2-N_2 interface the density and temperature behind the reflected and transmitted shocks and the vortex sheet strength for the equilibrium case, normalized by the frozen case, are plotted in Fig. 8. The differences due to dissociation occur at about $M = 6$. While the density and the temperature behind the reflected

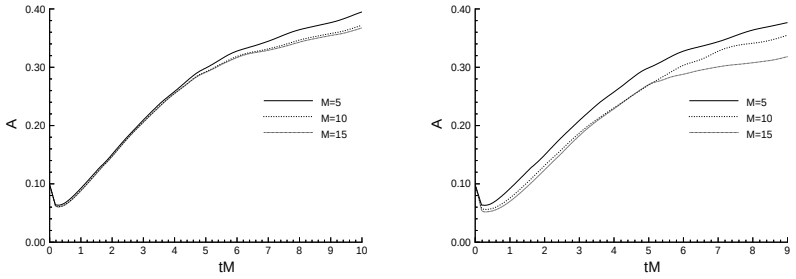

Figure 6: Amplitude of the perturbation as a function of scaled time (tM) for $M = 5, 10, 15$ shocks. The interface is a $A_0/\lambda = 0.1$, H_2-N_2 interface. (a) Frozen flow. (b) Equilibrium flow.

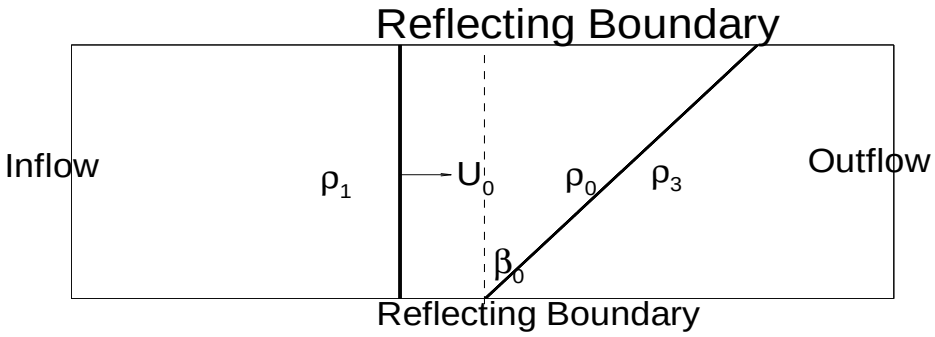

Figure 7: Schematic of a shock interaction with a sawtooth interface inclined at β_0 to the plane of the shock.

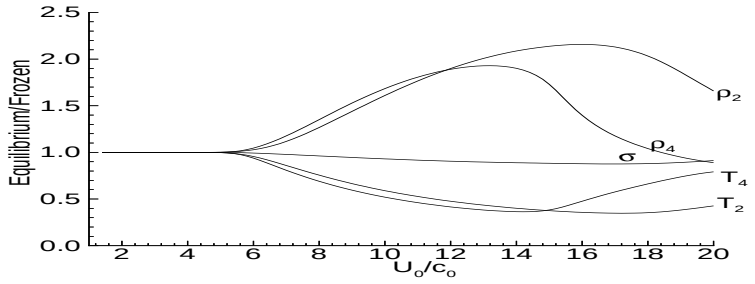

Figure 8: Local solution for equilibrium dissociated flow normalized by the frozen solution. Subscript '2' ('4') are for values between the reflected (transmitted) wave and contact surface. σ is the vortex sheet strength. $\beta_0 = 30°$, H_2-N_2 interface.

and the transmitted shock show appreciable differences due to dissociation, the change in the vortex sheet strength is small. These observations are consistent with those from the numerical simulations. For $M > 15$ all the diatomic species have dissociated completely and the resulting gas behaves as a monatomic perfect gas. This causes the reversal of the trends for the changes in density and temperature.

This analysis enables us to determine the initial baroclinic circulation generation on a sinusoidal interface by integrating the vortex sheet strength over the *original* length of the interface (see the horizontal curves in the circulation plot Fig. 5.

5 Conclusion

In this paper, we examined the effects of dissociation in the interaction of shocks with density interfaces under hypervelocity conditions. For the high Atwood number interfaces examined, chemical effects reduce the growth of the perturbations. A local analysis may be used to get the self-similar solution for weakly perturbed (small β_0) sawtooth interfaces. Furthermore, the local analysis shows that the change due to dissociation in the primary baroclinic vorticity generation is small for high Atwood number interfaces. A Mach number scaling was examined for strong shock cases. For the initial thermodynamic conditions examined, use of equilibrium chemistry models appears appropriate. The frozen limits will be achieved for extremely small, and hence impractical length scales. As a result of this study, it is apparent that for very strong shocks the linear regime of growth does not exist even for extremely small A_0/λ ratios.

References

[1] M. J. Lighthill, *Dynamics of a dissociating gas. part 1. equilibrium flow.*, J. Fluid Mech. **2** (1957), 1.

[2] P. F. Linden, D. L. Youngs, and S. B. Dalziel (eds.), *Proc. of the 4th International Workshop on the Physics of Compressible Turbulent Mixing.*, 1993.

[3] E. E. Meshkov, *Instability of the interface of two gases accelerated by a shock wave.*, Fluid Dynamics **4** (1969), 101, (translated from Izv. Akad. Nauk. SSSR, Mekh. Zhidk. Gaza, Vol. 5, pp. 151).

[4] D. I. Pullin, *Direct simulation methods for compressible ideal gas flow.*, J. Comput. Phys. **34** (1980), 231–244.

[5] R. D. Richtmyer, *Taylor instability in shock acceleration of compressible fluids.*, Comm. Pure and Appl. Math. **XIII** (1960), 297–319.

[6] R. Samtaney and N. J. Zabusky, *Circulation deposition on shock-accelerated planar and curved density-stratified interfaces: models and scaling laws*, J. Fluid Mech. **269** (1994), 45–78.